Food Chemistry: X 19 (2023) 100843

Contents lists available at ScienceDirect

Food Chemistry: X

journal homepage: www.sciencedirect.com/journal/food-chemistry-x

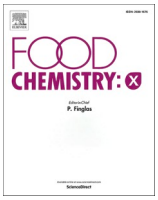

Insight into the differences of meat quality between Qinghai white Tibetan sheep and black Tibetan sheep from the perspective of metabolomics and rumen microbiota

Ying Ma, Lijuan Han *, Shutong Zhang, Xue Zhang, Shengzhen Hou, Linsheng Gui, Shengnan Sun, Zhenzhen Yuan, Zhiyou Wang, Baochun Yang

College of Agriculture and Animal Husbandry, Qinghai University Xining, 810016, People's Republic of China

ARTICLE INFO

Keywords:
Tibetan sheep
Meat quality
Sensory characteristics
Rumen microbiota
Metabolites

Chemical compounds studied in this article:
D-glucose 6-phosphate (PubChem CID: 439958)
D-Fructose-6-phosphate (PubChem CID: 69507)
D-Mannose-6-phosphate (PubChem CID: 65127)
D-erythrose 4-phosphate (PubChem CID: 122357)
L-carnitine (PubChem CID: 10917)
Histidine (PubChem CID: 6274)
Cholesterol (PubChem CID: 5997)
Chenodeoxycholate (PubChem CID: 10133)
Dihydroxyacetone phosphate (PubChem CID: 668)
Taurine (PubChem CID: 11231123)
Argininosuccinic acid (PubChem CID: 16950)

ABSTRACT

The purpose of this study was to investigate the differences in meat quality between two local breeds of Tibetan sheep, the White Tibetan sheep and the Black Tibetan sheep in Qinghai, and to search for metabolic mechanisms that produce meat quality differences by analyzing differential metabolites and key rumen microorganisms. The meat quality results showed that one breed, SG73, was superior to the other (WG). Further investigation identified differences in the composition of muscle metabolites and rumen microorganisms between the two Tibetan sheep breeds. It also regulates muscle tenderness, water retention, fat content and the composition and content of AA and FA through two major metabolic pathways, AA metabolism and carbohydrate metabolism. These findings could be beneficial for the development of breeding strategies for Tibetan sheep in Qinghai in the future.

1. Introduction

Tibetan sheep are a primitive breed of sheep living between 3000 and 5000 m above sea level on the Qinghai-Tibet Plateau (QTP) where they represent most of the local livestock. These sheep are an important pillar of Tibetan herdsmen's livelihood and also play a crucial role in the ecosystem of the Qinghai-Tibet Plateau (Jing et al., 2022) as, compared with other breeds of sheep, Tibetan sheep is characterized by non-smelling, tender, and juicy meat as well as elastic and lustrous wool fibers (Zheng et al., 2022). In addition, Tibetan mutton is a high-protein, low-fat meat variety, rich in amino acids and fatty acids (Jiao et al., 2020). In terms of wool color, Tibetan sheep can be divided into white and black sheep, with the latter being the most popular one in Guinan County, Hainan Tibetan Autonomous Prefecture, Qinghai Province. Previous studies have shown that animals of each color contain genes that control meat traits, thus causing the physical and chemical characteristics of meat, and eventually its quality, to be different (Gurgul et al., 2021; Han et al., 2015). In this context, it should be noted that in Qinghai, it is a long-held belief that the meat quality of black Tibetan sheep is much higher than that of the white sheep.

In a similar way to genomics and proteomics, metabolomics plays an integral role in systems biology. This approach focuses on small molecules of relative molecular weights<1500 Da and uses chromatographic and mass spectrometric techniques for their qualitative and quantitative

* Corresponding author.
E-mail address: 2016990034@qhu.edu.cn (L. Han).

https://doi.org/10.1016/j.fochx.2023.100843
Received 20 May 2023; Received in revised form 30 July 2023; Accepted 15 August 2023
Available online 16 August 2023

analysis in large batches (Calderón & Lämmerhofer, 2022). Depending on the technique applied, between 50 and 5000 different small molecule metabolites can be simultaneously identified from biological samples. Gene transcription directs protein synthesis which, in turn, regulates various biochemical reactions that occur continuously in living organisms in the form of enzyme reactions and metabolic pathways (Q. Li et al., 2014). Metabolomics can provide a real-time monitoring approach to determine the state of cells and the health of the body (Cabaton et al., 2018). Changes in metabolites can represent the final outcome in response to changes in gene levels, protease activity, gut microbiota, and the internal environment (Wikoff et al., 2009). Therefore, metabolomics can be understood to be the downstream science of genomics and proteomics, and is the closest to the phenotype (Fiehn, 2002).

The rumen of ruminants is a good natural habitat for anaerobic microorganisms to colonize, and also acts as a natural reactor for the effective degradation of polysaccharides in plant cell walls, which is accomplished by rumen microorganisms (Guo et al., 2022). Therefore, the abundance and community composition of rumen microorganisms influence the digestibility of feeds and the function in the rumen (Białek, Czauderna, & Białek, 2018) (Xing et al., 2020) (Cobellis, Trabalza-Marinucci, & Yu, 2016), which in turn has an important impact on the performance and meat quality of ruminants (Białek et al., 2018; Matthews et al., 2019). For example, the rumen cocci family would be involved in AA and FA metabolism and is a potentially beneficial bacterium (H. Li, Mi, Duan, Ma, & Fan, 2020). Dietary supplementation to increase rumen amylolytic bacteria associated with fatty acid synthesis can improve the meat quality of yaks (Du et al., 2021). Microorganisms in the rumen ultimately influence the meat quality of black Tibetan sheep by regulating metabolic pathways (X. Zhang, Han, Hou, Raza, Gui, et al., 2022). Numerous studies have shown that diet has a strong influence on rumen microbial populations (Guerreiro et al., 2022) (Shi et al., 2022) (Gui et al., 2021), but studies also been shown that there is different in rumen bacteria between different varieties of the same species (Xiang et al., 2022), and even that the influence of individual hosts is much greater than the influence of diet (Weimer, Waghorn, Odt, & Mertens, 1999).

Based on previous studies (X. Zhang et al., 2023) (X. Wang et al., 2022), we hypothesized that the composition of rumen microorganisms and muscle metabolites varied among the different breeds of Tibetan sheep, and that there may be an interaction between the two. Therefore, 16S rDNA amplicon sequencing technology was used to identify rumen microorganisms in samples and reveal their species composition. By comparing the data on microbial populations, the latter's functional profiles were also investigated. A high-resolution non-target metabolic technology, based on UHPLC-QTOF-MS, was subsequently applied to analyze all metabolites in the *longissimus dorsi* muscle of Tibetan sheep to differentially screen abundant metabolites as well as important metabolic pathways. Finally, targeted metabolic techniques, based on selective reaction (MRM), was performed to determine amino acid and fatty acid content to further verify and characterize these interactions. Correlations between intestinal differentially abundant microorganisms and muscle differential metabolites, as well correlations between these factors and meat quality were also carried out to identify relationships which would explain the meat quality differences between the two varieties (white and black Tibetan) sheep. This research is expected to provide reference information for the identification of local breeding varieties and improving meat nutritional quality of Tibetan sheep.

2. Materials and methods

2.1. Tibetan sheep and meat samples

All animal care and handling were approved by the Institutional Animal Care and Use Committee Guidelines of Qinghai University (protocol number 0515).

Twelve healthy and disease-free sheep of similar weight (18.00 ± 3.00 kg) and weaned for 100 days were randomly selected from the same pasture in Guinan County, Hainan Tibetan Autonomous Prefecture, Qinghai Province (six Tibetan white sheep labeled as the WG group, six Tibetan black sheep labeled as the SG73 group). The 2 groups of sheep were kept in separate pens in the same sheep barn, which was equipped with a sports field, sheltered from the wind, facing the sun, dry and well ventilated. The sheep were fed with fodder twice a day at 8:30 am and 16:30 pm respectively during the fattening period. The feeding process was carried out for 90 days after an initial adaptation period of seven days and throughout this experimental period. Based on the "Meat Sheep Feeding Standards" (NY/T 816–2004), the feed consisted of a mixture of concentrate and forage in a ratio of 7:3, with the composition and nutritional level of the concentrate shown in Table S1. The roughage, on the other hand, consisted of oat hay and silage corn in a ratio of 1:1.

At the end of the experiment, feed and water were withheld for 12 h (fasting) prior to slaughter in accordance with animal welfare procedures. The animals were then humanely slaughtered in a commercial abattoir by following standard procedures, with the slaughtering process and subsequent collection of the *longissimus dorsi* muscles (muscles between the 9th and 11th ribs on the back of the Tibetan sheep) and rumen fluid performed under strict supervision. After collection, samples were immediately stored at −80 °C until required for use. From each group, nine replicates were used for determining meat quality, six replicates were used for determining 16S rDNA sequencing and metabolomics analysis.

2.2. Sensory analysis of Tibetan sheep

Reference Standards (STANDARD & ISO, 2003), we invited 10 trained panelists to evaluate the meat samples (including five males and five females). Prior to the evaluation they were trained in sensory evaluation (Miller, 2023) and were familiar with the evaluation of meat products. Meat samples were steamed with reference to the method of Scott O (Knowles, Grace, Rounce, & Realini, 2020), muscles were placed in TUFflex^{TM} bags and steamed in boiling water until the internal temperature of the muscle reached 75 °C, inserted the thermometer probe (FlashCheck® Jumbo Display Auto-Cal Anti-Microbial Needle Tip Thermometer, UK) into the center of the meat to measure the temperature. The two sets of samples at the end of steaming were divided into ten portions and numbered, marked with a random three-digit code.

The evaluators sat in a controlled room where each team member had a separate booth and the environmental conditions are kept as constant as possible, with pure water and cookies provided as a palate cleanser between samples. During each session, two sets of samples were given to each member for scoring in a randomized manner. Sensory assessments were conducted over three weeks, each lasting 1.5–2 h. The evaluators rated the color, juiciness, aroma, taste, and texture of the sheep. The scoring criteria are shown in Table S2.

2.3. Analysis of the edible quality and conventional nutritional quality of meat

After thawing, the edible quality of Tibetan sheep samples was determined based on conventional methods, including pH_{24h}, WBSF (Warner-Bratzler shear force), cooked meat percentage, cooking loss, dripping loss and chromatic value (L* is luminosity, a* is red, and b* is yellow). The pH_{24h} was determined by completely embedding the electrode head of a calibrated pH meter into the meat sample (while avoiding fat and fascia) until it reached the center of the meat sample; the electrode was allowed to stand for>5 min to take the reading after it had stabilized (Devapriya et al., 2021). The WBSF was measured using a tenderizer by cutting in the direction perpendicular to the muscle fibers (meat-like size: 2 cm × 1 cm × 1 cm) (Atsbha, Gebremariam, & Aregawi, 2021). The cooked meat percentage, cooking loss and dripping loss were

determined with reference to the method of Honikel et al (Honikel, 1998). Finally, color differences of meat after natural oxidation in air for 15 min were determined using a corrected TCP_2 automatic colorimeter (L*, a*, b*) (Borges et al., 2014). All experiments were performed three to five times to determine the average values.

The water, protein, and fat contents of meat samples, indicative of the nutritional quality of the meat, were determined according to specified meat detection standards. Briefly, for the moisture content, the samples were heated in an oven at 150 ± 2 °C oven until the weight was constant. Similarly, the number of proteins was determined using the Kjeldahl method while the fat content was measured by extracting dry samples with petroleum ether in a Soxhlet extractor.

2.4. Targeted metabolomics profiling

2.4.1. Analysis of the composition and content of AA of meat

Two hundred microliters of water were added to 80 mg of sample and the mixture was homogenized, using a tissue homogeniser for 20 s (TissueMaster™). And adding 800 μL of a methanol/acetonitrile solution (1:1, v/v). After mixing for another 60 s with a vortex mixer, the samples were subjected to two low-temperature ultrasonications (4℃), each for 30 min. They were then kept at −20 °C for 1 h to precipitate protein prior to a 20 min centrifugation at 4 °C and 14 000 rcf. The supernatant was freeze-dried and stored at −80 °C. Samples were subsequently separated with an ultra-performance liquid chromatography (UPLC) system (Agilent 1290 Infinity LC) where the mobile phase A consisted of 25 mmol/L of Ammonium formate and 0.08% of FA aqueous solution while that of B consisted of 0.1% of FA acetonitrile. For the process, an automatic sampler at 4 °C was used, with the column temperature, flow rate and injection volume being 40 °C, 250 μL/min and 1 μL respectively. The gradient elution was performed as follows: for 0–12 min, a linear change in B from 90% to 70%; for 12–18 min, a linear change in B from 70% to 50%; for 18–25 min, a linear change in B from 50% to 40%; for 30–30.1 min, B was changed linearly from 40% to 90%; for 30.1–37 min, B was maintained at 90%. In the sample queue, a QC sample was periodically included alongside experimental ones to detect and evaluate the stability and repeatability of the system. Mass spectrometry was finally performed using a 5500 QTRAP mass spectrometer in positive-ion mode and under the following ESI source conditions: ion source temperature of 500 °C, ion source Gas 1 and 2 of 40 psi each, a curtain gas (CUR) of 30 psi, and an IonSpray Voltage Floating (ISVF) of 5500 V. The MRM mode was used to detect the ion pairs to be tested.

2.4.2. Analysis of the composition and content of FA of meat

After thawing on ice, 30 mg of sample were kept in a 2 mL glass centrifuge tube to which 1 mL of a chloroform/methanol solution was then added. The mixture was subsequently subjected to ultrasonication for 30 min and after adding 2 mL of a sulfuric acid–ethanol solution (1%), it was kept in a water bath for 30 min at 80 °C for methyl esterification. Extraction was then performed using 1 mL of *n*-hexane, with 5 mL of pure water subsequently added for washing. Twenty-five microliters of methyl *n*-octadecanoate was then added to 500 μL of this mixture as the internal standard. After mixing, the sample was separated by gas chromatography using an injection volume of 1 μL and a split ratio of 10:1. The temperature settings involved an initial temperature of 50 °C, held for 3 min, before raising it to 220 °C at a rate of 10 °C/min, and maintaining the new temperature for 5 min. Helium at a flow rate of 1.0 mL/min was used as the carrier gas. To evaluate the stability and repeatability of the system, a QC sample was included at intervals after a certain number of samples in the sample queue. This was followed by analysis using mass spectrometry where the temperature of the sample inlet, ion source, and transmission line were set to 280 °C, 230 °C and 250 °C respectively. An electron impact ionization (EI) source, a SIM mode, and an electron energy of 70 eV were also applied.

2.5. Quantification of rumen microbiota and analysis of bacterial diversity

2.5.1. DNA extraction and sequencing

The rumen fluid samples were thawed under running water (4℃). Based on the method of Zhang et al (X. Zhang et al.), Genomic DNA was extracted from the samples, and the purity and concentration of DNA were tested. Based on the selection of sequenced regions, PCR amplification of selected V3-V4 variable regions was performed using specific primers with Barcode and high-fidelity DNA polymerase amplification (J. G. Caporaso et al.). The PCR products were examined by 2% agarose gel electrophoresis, and samples with brighter main bands between 400 and 450 bp were selected for further experiments. Then, the mixed PCR products were purified with AxyPrep DNA Gel Extraction Kit (AXYGEN). Sequencing libraries were prepared using the NEBNext® Ultra™ DNA Library Preparation Kit (NEB, USA). Constructed libraries were quality-checked by Agilent Bioanalyzer 2100 and Qubit, and the libraries were sequenced on the machine after passing the quality control. Finally, the libraries were sequenced on the Illumina MiSeq 2500 platform to generate 250 bp/300 bp paired-end reads.

2.5.2. Sequencing information analysis

Based on the method of Wrightad et al (Wright André-Denis et al., 2004), the QIIME 1.8.0 software was used for initial quality control of raw sequences where low quality sequences were filtered and the barcodes as well as the primer sequences were removed. The UCLUST software in QIIME was then used to cluster the spliced sequences into operational taxonomic units (OTUs) at a 97 % cutoff value before selecting, as representative sequences, those with the highest relative abundance for each OTU, and the representative sequences of OTUs were further annotated with species, using the Silva database. We also identified shared genera between samples and presented them in a Venn diagram using R software to highlight their composition and proportions in each sample (Sun et al., 2017). A nonparametric test (ANOSIM) was used to evaluate the overall similarity of the two groups of experimental data, and to evaluate their similarity. In addition, QIIME was also used to determine the Alpha diversity metrics (J. Gregory Caporaso et al., 2010). Based on information obtained from 16*S* sequencing data regarding species composition, PICRUSt software was eventually used to compare the functional profiles of microorganisms between the two groups (Langille et al., 2013).

2.6. Untargeted metabolomics profiling

2.6.1. Extraction of metabolites and UHPLC-QTOF-MS analysis

Muscle samples were processed with reference to Zhang et al (X. Zhang, Han, Hou, Raza, Gui, et al., 2022) The samples were analyzed by LC-MS/MS using UHPLC system combined with a Q Exactive mass spectrometer and HILIC column. Phase A of the liquid chromatography was the water phase, in which 25 mmol/L ammonium acetate and 25 mmol/L ammonia were added, and phase B was acetonitrile. The following elution gradient was used: 0–0.5 min, 95% mobile phase B; 0.5–7 min, the mobile phase B changed linearly from 95% to 65%; 7–8 min, the mobile phase B changed linearly from 65% to 40%; 8–9 min, mobile phase B maintained at 40%; 9–9.1 min, the mobile phase B changed linearly from 40% to 95%; 9.1–12 min, mobile phase B maintained at 95%. The column temperature and automatic sampler temperature were set to 25 °C and 4 °C, respectively, and the injection volume was 2 μL. In order to prevent the fluctuation of the signal in the instrument detection from affecting the results, we used a random sequence to conduct continuous analysis of the samples. The primary and secondary mass spectrometry data were collected on an AB Triple TOF 6600 mass spectrometer after which the Triple TOF 6600 mass spectrometer (AB SCIEX) was used for mass spectrometry analysis. Mass spectrometry conditions: electrospray ion source (ESI); data-dependent acquisition (IDA); spray voltage, 5500 V and −4500 V (positive and

negative ion mode); first-order collision energy (MS1) of 10 eV and the second-order collision energy (MS2) of 35 ± 15 eV; decluttering voltage (80 V); air curtain gas (35 psi); atomizing gas (Gas 1–50 psi); auxiliary heating gas (Gas 2–50 psi).

2.6.2. Data analysis

All collected data were preprocessed by Peakview 2.2 software (AB Sciex, USA) to include baseline correction, peak extraction and peak alignment. This was followed by metabolite structure identification, data pre-processing of XCMS, data processing, evaluation of experimental data quality and finally data analysis. For multivariate analysis, principal component analysis (PCA) was used to analyze data quality control (QC) and quality assurance (QA). PCA was used to observe whether the WG group was distinct and clearly separated from the SG73 one. An OPLS-DA model was then constructed using the replacement test to prevent over-fitting of the model. Through this approach, a variable importance for projection (VIP) >1, a p-value<0.05 and a difference multiple FC>1.2 or<0.83 were selected as thresholds to screen potential markers that contributed to the separation of the two groups. Additionally, the metabolic pathways of differential metabolites were analyzed by the MetPA database based on KEGG pathway analysis (Kanehisa, 2019; Kanehisa, Furumichi, Sato, Ishiguro-Watanabe, & Tanabe, 2021; Kanehisa & Goto, 2000). Any significantly different metabolic pathway was annotated and used in a general relationship diagram between the metabolic pathways.

2.7. Statistical analysis and network analysis

For data analysis, Tibetan sheep were used as the experimental unit. Independent-samples t-tests of SPSS 20.0 (IBM Corporation, Armonk, NY, USA) software were used to analyze the differences in meat quality between the WG and SG73 groups. A *P*-value of < 0.05 was considered statistically significant. In order to determine the correlation between meat quality and muscle metabolites as well as correlations with rumen microbial composition, using Pearson's correlation coefficients to work visual correlation maps.

3. Results

3.1. Sensory analysis of meat

The sensory attributes of cooked Tibetan sheep samples were assessed by the trained panel; their results are shown in Fig. 1-a and Fig. 1-b. The mean scores for the three traits of juice leaching, fragrance, and taste overlapped, showing no significant difference between the meat samples of white Tibetan sheep and black Tibetan sheep ($P > 0.05$). However, in terms of color and qualitative structure, the SG73 group scored higher ($P < 0.05$) and had higher acceptability.

3.2. Edible quality and conventional nutritional quality of meat

Meat quality is crucial for the consumption of meat products. The indices normally used to measure meat quality include pH_{24h}, meat color, water holding capacity, and tenderness (expressed in terms of the shear force). As shown in Table 1, the pH_{24h} values of the two groups were in the standard range (5.6 ~ 6.4) and were not significantly different. But the WBSF, cooking loss, and drip loss, as well as the L* and b* values of SG73, were significantly lower than those of WG, and in the case of a*, the value was higher for SG73 ($P < 0.05$).

The main conventional nutrients for evaluating meat quality are water content, fat content, protein content, and other indicators. According to Table 1, the two groups Tibetan sheep did not differ significantly in water or protein content, but the fat content of the WG group was significantly higher than that of the SG73 group ($P < 0.01$).

Table 1
The difference in edible quality and conventional nutritional quality between white Tibetan sheep and black Tibetan sheep.

Parameters	Groups		SEM	P-value
	WG	SG73		
pH (24 $_h$)	5.79	5.77	0.06	0.752
WBSF (N)	25.84**	12.57	2.48	0.000
Cooked meat percentage (%)	71.67	77.78	0.00	0.053
Cooking loss (%)	35.26**	15.54	0.04	0.000
Drip loss (%)	11.28*	8.79	0.01	0.034
L*	33.13**	26.00	1.33	0.001
a*	10.78**	18.92	1.81	0.000
b*	12.36**	5.81	1.11	0.000
Fat (%)	4.44**	2.31	1.55	0.001
Protein (%)	20.02	21.76	2.99	0.228
Water (%)	74.84	73.49	1.71	0.096

*$P < 0.05$ and **$P < 0.01$ compared with the SG73 group, **represents a highly significant difference between the two groups, *represents a significant difference between the two groups. WG: white Tibetan sheep group, SG73: black Tibetan sheep group.

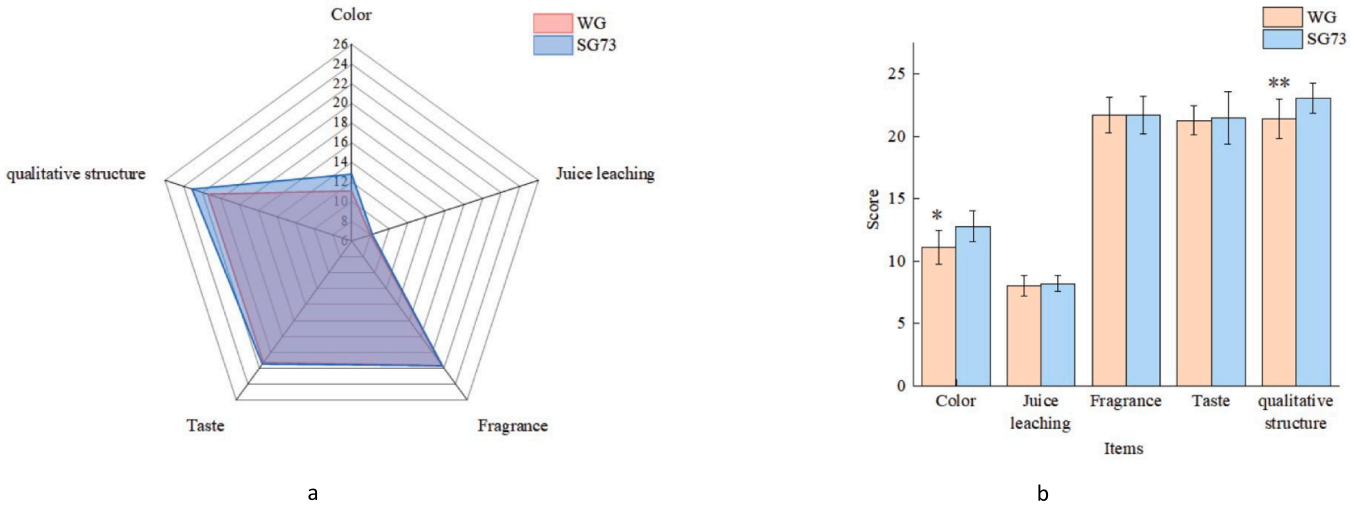

Fig. 1. Radar chart of sensory scores of white and black Tibetan sheep **(a)**, Histogram of sensory scores of white and black Tibetan sheep **(b)**. *$P < 0.05$ and **$P < 0.01$ compared with the SG73 group, **represents a highly significant difference between the two groups, *represents a significant difference between the two groups. WG: white Tibetan sheep group, SG73: black Tibetan sheep group.

3.3. Targeted metabolomics contouring (AA, FA and their derivatives)

The two groups of Tibetan sheep displayed significant differences in terms of amino acid composition and content (Table 2). The total amino acid (TAAs) and non-essential amino acid (NEAAs) content for the SG73 group were higher compared with those of the WG group, but the latter still had more essential amino acid (EAAs) ($P < 0.05$). In addition, the levels of glutamine, creatine, leucine, histidine, asparagine, hydroxyproline and creatinine were higher in the SG73 group ($P < 0.01$), and those of arginine, serine, and citrulline were also higher in SG73 ($P < 0.05$). At the same time, the concentrations of alanine, threonine, valine, glutamate, lysine, choline, isoleucine, aspartate, methionine, putrescine and cystine in the WG group were significantly greater than those in the SG73 group ($P < 0.05$).

The composition and content of fatty acids are shown in Table 2. No differences were found in the saturated (SFA) and monounsaturated fatty acids (MUFA) content between the two groups. However, while the amount of polyunsaturated fatty acids (PUFA) and the n-6 series ones was lower in SG73, this group had a higher concentration of n-3 series ($P < 0.05$). In addition, C18:1TN9, C18:2TTN6 and C24:1N9 were not detected for SG73, but the contents of C20:3N3, C20:5N3, C21:0, C24:0 and C23:0 were higher for SG73 ($P < 0.05$). As far as the WG group was concerned, the C18:2N6, C20:4N6, C22:3N6, C20:3N6, C22:0 and C22:5N6 was higher compared with the SG73 group ($P < 0.05$). It is worth noting that the n-6/n-3 percentage was also significantly higher in the WG group ($P < 0.01$).

3.4. Rumen microbiota

3.4.1. Sample diversity

A total of 4289 OTUs were identified in the two groups, of which 1700 and 838 specific OTUs were identified in the WG and SG73 groups, respectively (Fig. 2-a). The dilution curve of each sample approached a flattened shape, indicative of adequate sequencing (Fig. 2-b). Regarding the α diversity metrics of ruminal microbiota (Table S3), based on OTU and species abundance, the results showed no differences in the indices (Sobs, Shannon, Simpson, Chao1, Ace) of the two groups ($P > 0.05$). Anosim analysis is a non-parametric test, based on Bray-Curtis algorithm, that helps to determine whether differences between groups are significantly greater than within group variations. In this case, the R value can vary between −1 and 1, with values>0 indicating significant between-group differences (Fig. 2-c). Meanwhile, both hierarchical cluster analysis of samples further confirmed that the intestinal microbiota compositions of the WG and SG73 groups were different (Fig. 2–d and Fig.S1).

3.4.2. Species annotation and classification

T-test-based comparisons between the two groups were performed at the phylum and genus levels. In the former case, the rumen microbiota of the two groups of Tibetan sheep were mainly composed of *Bacteroidetes* and *Firmicutes* (Fig. 3-a). Compared with WG, *Bacteroidetes* of the SG group showed an upward trend, while *Firmicutes* showed a downward trend. A total of 118 bacterial groups with a relative abundance of $> 0.1\%$ were identified at the genus level, with the first 10 genera having a relatively high abundance (Fig. 3-b). Moreover, 20 differentially abundant genera were identified based on Welch's *t*-test (Fig. 3-c). These included *Christensenellaceae R-7 group, Mogibacterium, Alistipes and Odoribacter*, more abundant in the SG73 group ($P < 0.05$). For the WG, *Allobaculum, Phascolarctobacterium, Blautia, Ruminiclostridium 5, Lachnoclostridium, Saccharofermentans, Erysipelatoclostridium, Akkermansia et al* were more abundant ($P < 0.05$). The results of the rumen microbiota compositions allowed the identification of the functional profiles of the populations, "Amino Acid Metabolism" and "Carbohydrate Metabolism" were identified as the two most important functions of the rumen microorganisms (Fig. 3-d).

Table 2
The differences in the composition and content of AA, FA and its derivatives between white Tibetan sheep and black Tibetan sheep.

parameters	Groups		SEM	P-value
	WG	SG73		
AA (umol/g)				
glutamine	0.61**	8.30	1.06	0.002
creatine	3.25**	8.02	0.18	0.000
alanine/sarcosine	8.29**	6.09	0.23	0.001
arginine	0.43*	0.62	0.05	0.019
leucine	0.38**	0.57	0.02	0.001
threonine	0.84*	0.48	0.08	0.014
serine	0.48*	0.53	0.02	0.036
valine	0.55*	0.46	0.02	0.018
histidine	0.20**	0.44	0.04	0.003
glutamate	0.85*	0.32	0.12	0.012
lysine	0.39*	0.31	0.03	0.033
asparagine	0.11**	0.33	0.03	0.002
citrulline	0.07*	0.25	0.04	0.015
hydroxyproline	0.17**	0.28	0.01	0.000
choline	2.58**	0.21	0.24	0.001
isoleucine	0.25**	0.18	0.01	0.000
creatinine	0.09**	0.12	0.01	0.006
aspartate	0.24**	0.06	0.03	0.005
methionine	0.16**	0.04	0.01	0.000
putrescine	0.01**	0.00	0.00	0.006
cystine	0.02*	0.00	0.01	0.017
EAAs[1]	3.06*	2.50	0.16	0.024
NEAAs[2]	26.21*	39.16	3.04	0.013
TAAs[3]	31.87*	41.88	3.20	0.035
FA (ug/g)				
C18:2N6	672.04*	520.10	37.34	0.015
C20:4N6	226.50**	2.81	2.81	0.000
C22:6N3	157.75**	6.77	23.33	0.003
C20:2N6	44.61**	0.00	0.56	0.000
C20:3N6	22.08	2.81	1.19	0.046
C18:1TN9	31.61*	0.00	6.88	0.044
C22:0	17.09**	1.51	0.72	0.000
C18:2TTN6	11.18**	0.00	1.78	0.003
C24:1N9	10.84**	0.00	0.41	0.000
C22:5N6	8.73**	8.02	0.10	0.002
C20:3N3	3.08**	187.83	1.21	0.000
C20:5N3	1.65**	14.40	0.73	0.000
C21:0	1.06**	3.61	0.18	0.000
C24:0	0.67**	1.60	0.14	0.003
C23:0	0.50*	0.88	0.10	0.017
SFA[4]	2314.83	3010.23	1033.57	0.538
MUFA[5]	2435.87	2839.16	850.60	0.660
PUFA[6]	1263.79*	858.35	43.59	0.011
n-3[7]	237.37*	274.63	18.84	0.119
n-6[8]	1026.42**	583.73	40.38	0.000
n-6/n-3	4.38**	2.12	0.40	0.005
C16:0/C18:1	0.56	0.58	0.03	0.649

*$P < 0.05$ and **$P < 0.01$ compared with the SG73 group. **represents a highly significant difference between the two groups, *represents a significant difference between the two groups. WG: white Tibetan sheep group, SG73: black Tibetan sheep group.

[1] EAAs = (leucine + methionine + valine + isoleucine + threonine + phenylalanine + lysine + tryptophan). EAAs: essential amino acids;

[2] NEAAs: nonessential amino acids;

[3] TAAs: total amino acids.

[4] SFA = (C22:0 + C10:0 + C16:0 + C15:0 + C17:0 + C14:0 + C13:0 + C11:0 + C8:0 + C21:0 + C18:0 + C12:0 + C24:0 + C23:0 + C20:0), saturated fatty acids.

[5] MUFA = (C18:1TN9 + C17:1N7 + C16:1N7 + C15:1N5 + C22:1N9 + C18:1N9 + C20:1N9 + C14:1N5 + C24:1N9), monounsaturated fatty acids.

[6] PUFA = (C20:2N6 + C22:4N6 + C20:3N3 + C18:2N6 + C22:2N6 + C22:6N3 + C18:3N6 + C20:3N6 + C18:3N3 + C18:2TTN6 + C20:4N6 + C22:5N3 + C20:5N3 + C22:5N6), polyunsaturated fatty acids.

[7] n-3 = (C20:3N3 + C22:6N3 + C18:3N3 + C22:5N3 + C20:5N3), omega-3 polyunsaturated fatty acids.

[8] n-6 = (C20:2N6 + C22:4N6 + C18:2N6 + C22:2N6 + C18:3N6 + C20:3N6 + C18:2TTN6 + C20:4N6 + C22:5N6), omega-6 polyunsaturated fatty acids.

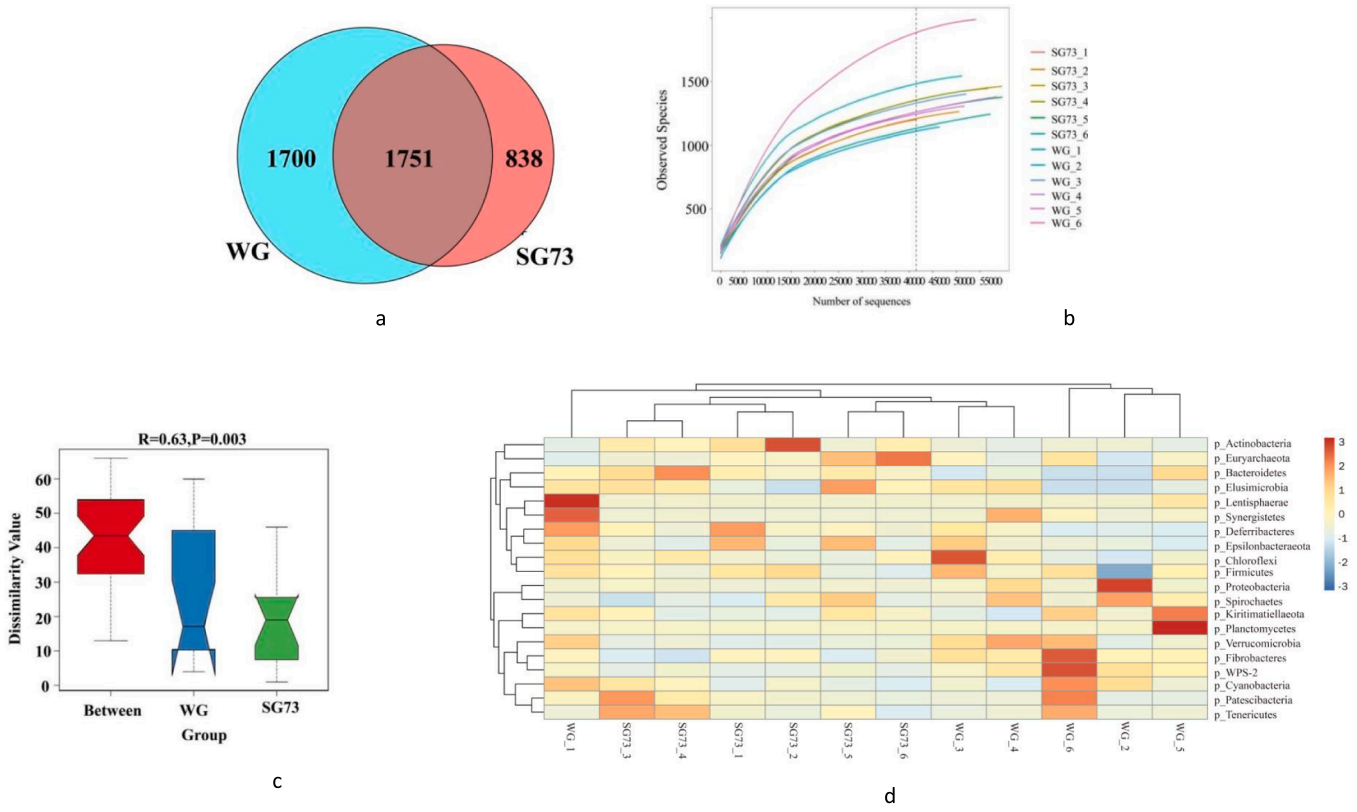

Fig. 2. OTU Venn**(a)**; Rarefaction Curve**(b)**; Differences between Anosim groups**(c)**. Heat map of species abundance clustering at each sample phylum level**(d)**.

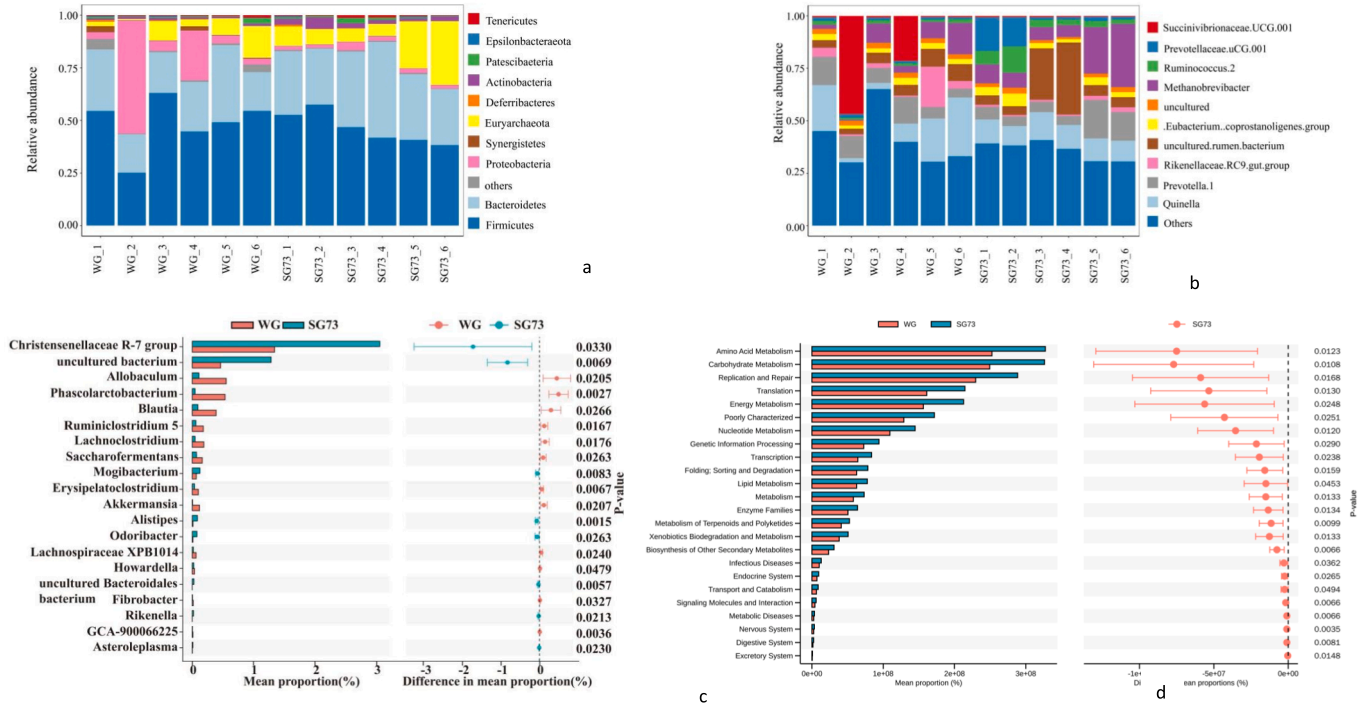

Fig. 3. Relative abundance of bacteria community proportions at the phylum**(a)**; Relative abundance of bacteria community proportions at the genus**(b)**; Indigenous differential ruminal microbial at genus level**(c)**; Predicted differential ruminal microbial functions**(d)**. Figure c and d show the proportion of abundance of different rumen bacteria and functional entries in the two groups of samples, respectively, and in the middle, the proportion of differences within the 95% confidence interval. The rightmost value is the p-value, and a $P < 0.05$ indicates a significant difference.

3.5. Untargeted metabolomic analysis

3.5.1. Untargeted metabolites

The spectral overlap comparison of the total ion flow diagrams of QC samples showed that the response intensities and retention times of the peaks basically overlapped, and the variation caused by the instrument errors was small throughout the experiment (Fig.S2). The metabolic profiles of all Tibetan sheep samples were analyzed by unsupervised PCA, and the profiles of each group, under the positive ion mode (Fig.S3-a) were obtained. It was observed that the WG group could be clearly distinguished from SG73, indicating physiological and metabolic differences between the two groups. To improve the separation of the groups, the QC samples were removed prior to additional analysis involving PLS-DA and OPLS-DA pattern recognition methods. The results showed that WG and SG73 were distributed on both sides of the PLS-DA (Fig.S3-b) and the OPLS-DA score maps (Fig.S3-c), respectively. thereby reflecting intra-group aggregation as well as inter-group separation. To ensure the effectiveness of the model and prevent its overfitting during the modeling process, permutation tests were used to test the model, with Fig.S3-d and Fig.S3-e representing the PLS-DA ($R^2X = 0.349$, $R^2Y = 0.988$, $Q^2 = 0.832$) and OPLS-DA replacement test diagrams ($R^2X = 0.349$, $R^2Y = 0.988$, $Q^2 = 0.69$) of the WG and SG73 groups respectively. With a gradual decrease of the replacement retention, the R^2 and Q^2 of the random model decreased, hence indicating the absence of over-fitting in the original model as well as its robustness. As shown in Table 3, the use of a VIP value > 1 alongside independent sample t-tests can help to screen significant differential metabolites. Through this approach, the positive ion detection mode successfully identified 49 differential metabolites, of which 25 were associated with KEGG metabolic pathways. These included carbohydrates (D-glucosaminic acid, stachyose, isomaltose, D-fructose-6-phosphate, D-mannose-6-phosphate, D-glucose 6-phosphate), amino acids and derivatives (L-carnitine, 5-aminovaleric acid, taurine, histidine, L-hydroxyarginine, *cis*-13-docosenoic acid, argininosuccinic acid), fatty acids and derivatives

Table 3
The detailed results of differential metabolites in the *longissimus lumborum* in the positive ion detection mode (OPLS-DA VIP > 1 and P value < 0.05)(WG vs SG73).

Name	Adduct	*m/z*	Rt(s)	VIP	FC	Variation
Pipamperone	[M + H] +	376.26	34.56	2.22	5.91	↑
Chenodeoxycholate	[M + H] +	393.28	34.42	1.45	4.94	↑
D-glucosaminic acid	[M + H-H_2O] +	178.08	296.65	3.17	5.67	↑
2-despiperidyl-2-(5-carboxypentylamine) repaglinide	[M + H-$C_{16}H_{21}NO_4$] +	194.12	213.25	1.35	2.17	↑
5-aminovaleric acid	[M + H] +	118.09	396.20	1.02	1.81	↑
3,4-dimethylphenyl methylcarbamate	[M + H] +	180.10	232.02	2.16	6.71	↑
Calcitriol	[M + H-3H_2O] +	363.29	36.14	1.11	2.45	↑
L-palmitoylcarnitine	[M + H] +	400.34	177.44	6.23	3.16	↑
3-hydroxyhexadecanoylcarnitine	[M + H] +	416.34	200.91	4.79	3.54	↑
1-(1z-hexadecenyl)-*sn-glycero*-3-phosphocholine	[M + H] +	480.34	189.75	4.13	1.92	↑
Glycerophosphocholine	[M + H] +	258.11	387.14	11.21	0.42	↓
L-carnitine	[M + H] +	162.11	367.06	24.86	1.27	↑
Taurine	[M + H] +	126.02	304.39	10.41	0.50	↓
Sulfamethazine	[M + H] +	279.08	416.51	2.89	1.47	↑
Oleoyl-l-carnitine	[M + H] +	426.36	174.07	7.93	2.20	↑
Thr-His	(M + CH_3CN + H) +	298.15	447.83	1.32	3.63	↑
1-palmitoylglycerol	[M + H-H_2O] +	313.27	33.56	1.77	1.17	↑
Histidine	[M + H] +	156.08	457.07	2.74	1.28	↑
His-Val	[M + H] +	255.14	445.04	5.45	2.13	↑
Palmitoyl sphingomyelin	[M + H] +	703.57	183.75	4.64	1.40	↑
Stachyose	(M + NH_4) +	684.25	489.53	1.21	0.04	↓
2-(3,4-dihydroxyphenyl) ethyl(1 s,4ar,7ar)-4a-hydroxy-7-methyl-5-oxo-1-[(2 s,3r,4s,5s,6r)-3,4,5-trihydroxy-6-(hydroxymethyl) oxan-2-yl]oxy-1,6,7,7a-tetrahydrocyclopenta[*c*]pyran-4-carboxylate	[M + H] +	527.15	453.84	1.19	0.03	↓
Cholesterol	[M + H-H_2O] +	369.35	32.91	2.57	1.61	↑
1-Stearoyl-2-oleoyl-*sn*-glycerol 3-phosphocholine (SOPC)	[M + H] +	788.61	41.56	4.55	0.80	↓
Isomaltose	[M + NH_4] +	360.15	397.74	2.06	0.10	↓
Edifenphos	[M + H-C_2H_4] +	283.02	471.55	3.71	0.54	↓
Lauroyl-l-carnitine	[M + H] +	344.28	187.75	1.97	3.24	↑
4,4′-methylenebis(2,6-di-*tert*-butylphenol)	[M + NH_4] +	442.35	196.94	4.15	2.09	↑
Clomazon	[M + H] +	240.10	227.81	3.02	0.20	↓
L-hydroxyarginine	[M + H-CH_5ON_3] +	116.07	324.53	2.37	0.70	↓
Cis-13-docosenoic acid	[M + H-H_2O] +	321.31	34.31	1.37	0.56	↓
Ala-Gln	[M + H] +	218.11	423.71	1.90	1.40	↑
Linoleoylcarnitine	[M + H] +	424.34	175.67	2.62	1.55	↑
N-(octadecanoyl) sphing-4-enine-1-phosphocholine	[M + H] +	731.61	181.88	5.48	1.51	↑
1,2-dioleoyl-*sn-glycero*-3-phosphatidylcholine	[M + Na] +	808.58	40.53	2.65	0.83	↓
3-hydroxyoleylcarnitine	[M + H] +	442.35	160.85	1.29	1.75	↑
1-o-hexadecyl-2-o-(4z,7z,10z,13z,16z,19z-docosahexaenoyl)-*sn*-glyceryl-3-phosphorylcholine	[M + H] +	792.59	40.13	1.91	1.40	↑
Erucamide	[M + H] +	338.34	34.29	9.01	0.57	↓
D-Fructose-6-phosphate	(M + NH_4) +	278.06	454.14	1.04	0.51	↓
D-Mannose-6-phosphate	(M + H-2H_2O) +	225.02	472.00	3.85	0.55	↓
Larixinic Acid	(M + H) +	127.04	471.54	3.23	0.55	↓
3-hydroxy-3-methylglutaric acid	[M + H-3H_2O] +	109.03	454.27	1.90	0.51	↑
L-arachidonoylcarnitine	[M + H] +	448.34	43.98	1.02	1.44	↑
D-glucose 6-phosphate	[M + H] +	261.04	471.12	6.07	0.50	↓
Argininosuccinic acid	[M + H] +	291.13	475.98	1.39	0.61	↓
L-n5-(1-imino-3-pentenyl) ornithine	[M + H-NH_3] +	197.13	255.92	1.06	0.38	↓
1,2-dipalmitoleoyl-*sn-glycero*-3-phosphocholine	[M + H] +	730.54	152.48	1.20	0.11	↓
1-o-hexadecyl-2-o-(5z,8z,11z,14z,17z-eicosapentaenoyl)-*sn*-glyceryl-3-phosphorylcholine	[M + H] +	766.57	141.79	5.71	1.47	↑
Stearoylcarnitine	[M + H] +	428.37	132.48	3.43	5.16	↑

(L-palmitoylcarnitine, glycerophosphocholine, cholesterol, N-(octadecanoyl) sphing-4-enine-1-phosphocholine, 3-hydroxy-3-methylglutaric acid), the intermediate metabolites of nucleotides(sulfamethazine), and other organic compounds (chenodeoxycholate, 3,4-dimethylphenyl methylcarbamate, calcitriol, 4,4′-methylenebis(2,6-di-*tert*-butylphenol), edifenphos, clomazon). Of these metabolites, 13 were up-regulated in and 12 were down-regulated in the WG group compared with the SG73 group. The information on the differential metabolites in negative ion detection mode is shown in Table S3.

3.5.2. Functional annotation of the differential metabolites

After the integration of differential metabolites screened under positive and negative ion modes, KEGG pathway annotation and analysis were performed. Among these, Carbohydrate metabolism, Lipid metabolism, Membrane transport, Energy metabolism, Signal transduction, Global and overview maps, Digestive system, and Cell growth and death were the major pathways affected by the Tibetan sheep breed (Fig. 4-a). Differential abundance scores can capture the average and overall changes of all metabolites in a certain pathway (Fig. 4-b). This identified necroptosis, cholesterol metabolism, the sphingolipid signaling pathway, bile secretion, sphingolipid metabolism, secondary bile acid biosynthesis, and the neurotrophins signaling pathway as the major up-regulated metabolic pathways. Similarly, the down-regulated metabolic pathways included galactose metabolism, glycerophospholipid metabolism, carbon fixation in photosynthetic organisms, carbohydrate digestion and absorption, starch and sucrose metabolism, glycerolipid metabolism, inositol phosphate metabolism, carbon metabolism, ether lipid metabolism, methane metabolism, lysosome, ABC transporters, and the PTS (phosphotransferase system).

As shown in the Fig-S4, fat deposition in the muscle of the WG group may be due to the upregulation of the bile secretion pathway, which in turn promotes fat digestion and absorption (Fig-S5). In addition, four metabolites including dihydroxyacetone phosphate, D-erythrose 4-phosphate, histidine, and Argininosuccinic acid were involved in the biosynthesis of amino acids and influenced the production of some downstream amino acids as shown in the Fig-S6. Meanwhile, the amino acid differences were reflected in the upregulated ABC transporters in the SG73 group (Fig-S7). Interestingly, the D-Mannose-6-phosphate and D-glucose 6-phosphate were enriched in the SG73 group, probably due to the up-regulation of the phosphotransferase system (PTS) pathway in the SG73 group (Fig-S8).

3.5.3. Correlational analysis between intestinal microbiota, muscle metabolites and meat quality

The correlation between meat quality, rumen microorganisms and targeted metabolomics results was analyzed (Fig. 5-a, Fig. 5-b). The results of the study showed a strong correlation between them. Among them, TAA, N-3 series fatty acids, and cooking loss were positively correlated with D-lactose, Taurine, *Odoribacter* and *Mogibacterium*, and negatively correlated with Cholesterol and Chenodeoxycholate. WBSF and Fat content were positively correlated with Cholesterol, Chenodeoxycholate, *Blautia*, *Erysipelatoclostridium* and negatively correlated with D-lactose and *Mogibacterium*. EAA, PUFA, and Drip loss were positively correlated with Cholesterol, chenodeoxycholate, L-carnitine, Histidine, *Phascolarctobacterium, Lachnoclostridium, Akkermansia, Erysipelatoclostridium, Blautia* and *Ruminiclostridium 5,* and negatively correlated with D-glucose 6-phosphate, D-Fructose-6-phosphate, D-Mannose-6-phosphate, Argininosuccinic acid, D-erythrose 4-phosphate, Dihydroxyacetone phosphate, *Christensenellaceae R-7 group* and *Alistipes.* L* was positively correlated with L-carnitine, chenodeoxycholate and *Blautia,* and negatively correlated with D-Mannose-6-phosphate, D-Fructose-6-phosphate, D-glucose 6-phosphate, Taurine, *Alistipes* and *Christensenellaceae R-7 group.*

In the analysis of the correlation between muscle metabolites and rumen microorganisms, the *Akkermansia*, *Saccharofermentans*, *Lachnoclostridium* and *Phascolarctobacterium* were positively correlated with L-carnitine, Histidine and Chenodeoxycholate. *Blautia* were positively correlated with L-carnitine, Histidine, Cholesterol and Chenodeoxycholate. *Erysipelatoclostridium* were positively correlated with Cholesterol and Chenodeoxycholate. *Christensenellaceae R-7 group* and *Alistipes* were positively correlated with D-Mannose-6-phosphate, D-Fructose-6-phosphate, D-erythrose 4-phosphate, D-glucose 6-phosphate, Dihydroxyacetone phosphate, Taurine and Argininosuccinic acid. In addition, *Lachnoclostridium* and *Blautia* were negatively correlated with D-

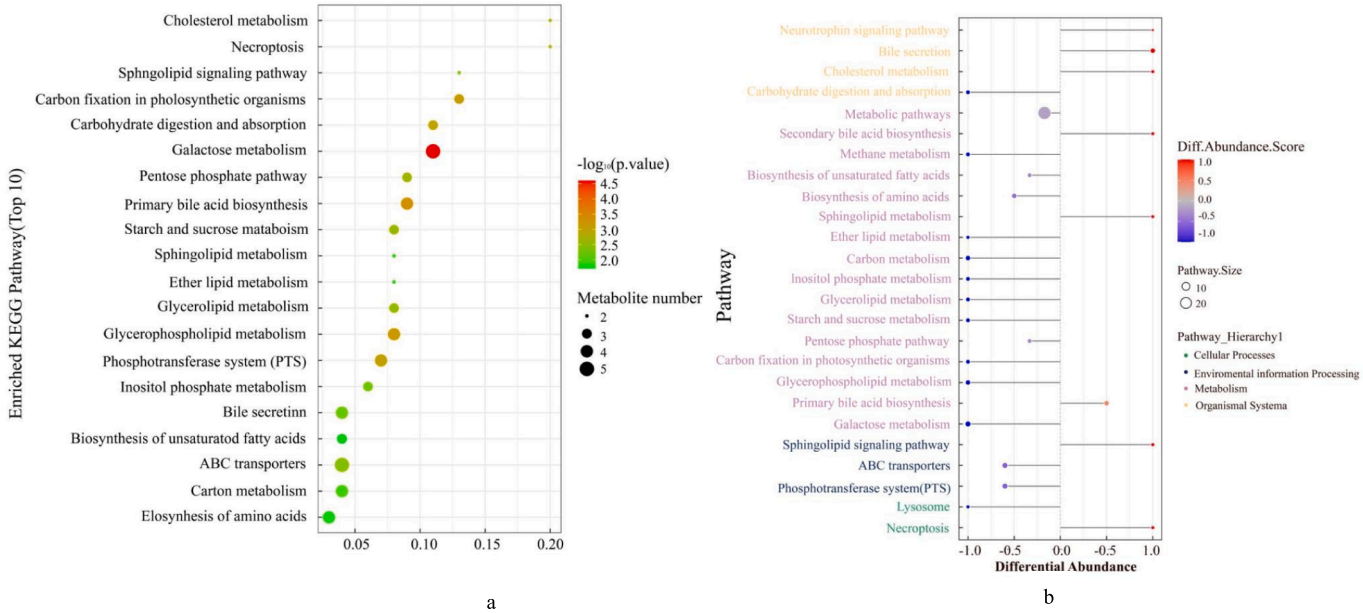

Fig. 4. KEGG pathway enrichment of differential metabolites in the *longissimus lumborum* of Tibetan sheep**(a)**. In the bubble diagram, each bubble represents a metabolic pathway. The larger the bubble is, the greater the impact factor is; the darker the bubble is, the more significant the degree of enrichment is. A differential abundance score map of differential metabolic pathways**(b)**. The differential abundance score captures the average, gross changes for all metabolites in a pathway. A score of 1 indicates an upward trend in all identified metabolites in this pathway, and − 1 indicated that the expression trend of all identified metabolites in this pathway was down-regulated in the WG group.

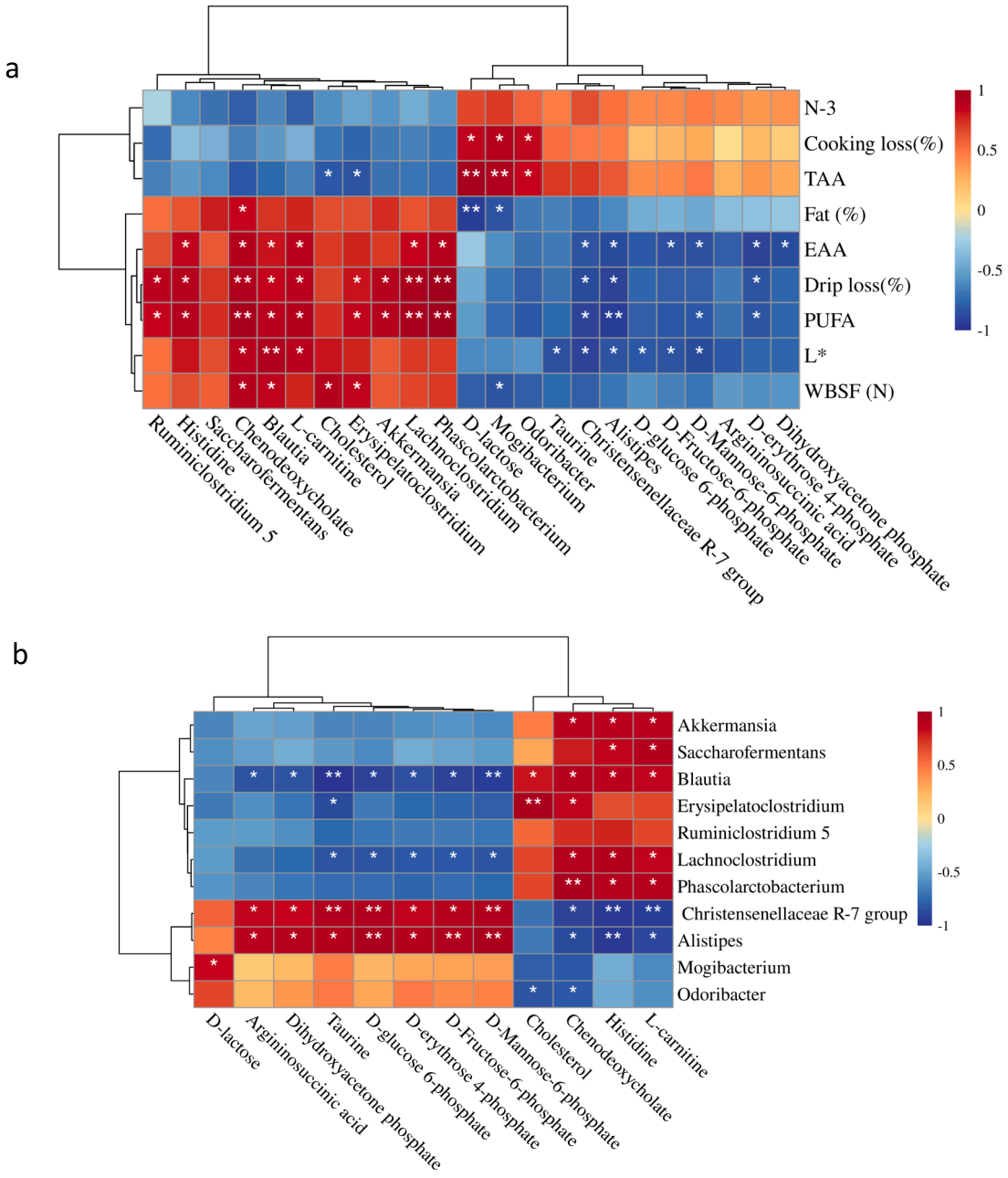

Fig. 5. Correlation heat map of Meat Quality with Muscle Differential Metabolites and Rumen Microorganisms **(a),** Correlation heat map of Rumen Microorganisms and Muscle Differential Metabolite**(b)**, The color red and blue represent positive and negative correlation, respectively, and the depth of the color indicates the correlation strength.

Mannose-6-phosphate, D-Fructose-6-phosphate, D-erythrose 4-phosphate, D-glucose 6-phosphate, Dihydroxyacetone phosphate, Taurine and Argininosuccinic acid. *Christensenellaceae R-7 group* and *Alistipes* were negatively correlated with L-carnitine, Histidine and Chenodeoxycholate.

4. Discussion

The sensory attributes of meat are important for consumer acceptance, while meat tenderness and flavor are important components of meat palatability (Miller, 2023; Scott, 1939). In this study, we found that the meat of white and black Tibetan sheep differed mainly in color and texture. This is generally consistent with the differences presented by our measured epistatic characteristics (WBSF, L*, a*, b*). The percentage of intramuscular fat positively influenced the juiciness and tenderness of the meat (Thompson, 2004), and studies have found that 4–5% intramuscular fat content is required to satisfy Australian consumers' satisfaction with palatability (Tian, Decker, & Goddard, 2013). In contrast, the results of this study showed that black Tibetan sheep with better tenderness had only 2% muscle fat. This result may be due to the specificity of the muscle fiber structure of black Tibetan sheep and the changes that occur in the muscle during steaming, and requires further investigation. Generally. after low-temperature steaming, the sheep surface is moist and the meat is pink with minimal change to brown (Ayub & Ahmad, 2019). The denaturation of myoglobin is important for the change of meat color, and the difference in color presented by the two groups of Tibetan sheep may be caused by the difference in the ratios of myoglobin (Arena, Salzano, Renzone,

D'Ambrosio, & Scaloni, 2014).

The tenderness of meat was characterized by shear force, which reflected the hardness, cohesion, and elasticity of the muscles to a certain extent. The shear force value of meat in the SG73 group was less than that in WG. Since a smaller shear force between muscles indicate thinner muscles, so the SG73 group showed better tenderness (Colucci, Macleod, Grovum, McMillan, & Barney, 1990). Studies have shown that accelerating the glycolytic metabolic pathway facilitates ATP production and glycogen degradation in postmortem muscle, which affects the rate of pH decrease, further affecting meat tenderness, color and juiciness (Chen et al., 2022). In the correlation analysis, WBSF was positively correlated with D-glucose 6-phosphate, and the up-regulated D-glucose 6-phosphate in the SG73 group may accelerated glycolysis by regulating the Starch and sucrose metabolism pathway, which may explain the more tender meat of SG73. Interestingly, Zhang et al (X. Zhang et al., 2023) reported that D-glucose 6-phosphate accumulation was able to reduce hexokinase activity, inhibit glycolysis, and slow down the rate of pH decrease. Additionally the translocation and phosphorylation of the PTS carbon source reduces the phosphorylation of glucose PTS (Phosphotransferase system), which decreases the activity of adenylate cyclase and therefore the cAMP concentration (Hogema et al.). This reduces glycogen metabolism by inhibiting phosphorylation of the APK (camp-dependent protein kinase) signaling pathway and glycogen phosphorylase (X. Zhang, Han, Hou, Raza, Wang, et al., 2022) Therefore, it is speculated that in the SG73 group glycolysis was inhibited by PTS upregulation and D-glucose 6-phosphate deposition, and the already ongoing glycolysis was accelerated by Starch and sucrose metabolism upregulation, thus delaying the pH reduction, but further proof is needed.

Muscle color can also reflect the degree of oxidation of muscles (Purslow, Gagaoua, & Warner, 2021). Liu et al (Liu et al., 2021) mentioned that myoglobin could be used as a selection parameter for the genetic improvement of meat color, oxidation of myoglobin results in the production of oxy-myoglobin, which leads to an increase in a* values. The correlation between flesh color and muscle water holding capacity was mentioned in the article by Zhang et al (X. Zhang et al., 2023). where L* and water holding capacity were positively correlated, which is consistent with the results of this paper. In addition, the muscle water holding capacity was correlated with the rate of pH decrease (Qiao, Fletcher, Smith, & Northcutt, 2001), and the reduction in cooking loss also could have been due to changes in the structure of myofibers which improved the water retention of muscle proteins (Palka & Daun, 1999). In the correlation analysis, there was a strong correlation between WBSF, L*, and cooking loss and D-glucose 6-phosphate, indicating that meat quality would be regulated by the glycolytic pathway. In the current study, the luminance (L*) and redness (b*) of the SG73 group were lower than those of the WG group, and the cooking loss and drip loss were also lower than those of the WG group. The above comprehensive analysis therefore showed that meat from black Tibetan sheep was of better edible quality.

Excessive accumulation of cholesterol can disrupt normal cholesterol metabolism in animal livers, resulting in hypercholesterolemia and fatty deposits (Zheng et al., 2022). In contrast, n-3 fatty acids can reduce fat deposition in adipose tissue by inhibiting lipase and increasing beta oxidation, which is also important for controlling cholesterol synthesis (Harlioğlu et al., 2012). This study found that the higher n-3 series fatty acid content in the SG73 group could only be the reason for its lower fat content. In contrast, for the WG group, the upregulated cholesterol as well as the cholesterol metabolic pathway were potential markers of its fat deposition. But L-carnitine, an amino acid that promotes the conversion of fat into energy, can bind to acyl-coenzyme A to transfer long-chain fatty acids from the cytoplasmic matrix into the mitochondrial matrix for subsequent β oxidation (Sadet-Bourgeteau, Martin, & Morgavi, 2010), in the WG group, L-carnitine is adjusted upward. In addition, Ley et al (Ley, Turnbaugh, Klein, & Gordon, 2006) reported the relationship between human gut microbial ecology and body fat and showed that a higher proportion of thick-walled bacteria as well as fewer anaphylactic bacteria were contained in the obese population, which is consistent with our findings. It suggests that changes in the gut microbiota may be one of the factors affecting fat deposition in animals.

Different breeds of sheep have different nutrient compositions, metabolites, and rumen bacterial communities (Xiang et al., 2022), we also get the same results. The first is the difference in AA, SG73 group has higher TAA. The type and composition of amino acids have a greater impact on the quality of meat, such as glutamic acid, arginine, aspartic acid, alanine and glycine acting as important prerequisites for volatile flavor compounds that affect the flavor of meat (Lee, Kwon, Kim, & Kim, 2011). Creatine is a nitrogen-containing organic acid that provides energy to the muscles (Stahl et al., 2007), while Glutamine can stabilize the color of meat by stimulating mitochondrial respiration (Egelandsdal, Berg, Wahlgren, & Slinde, 2016). Leucine couples to myogenic regulatory factor genes via the AKT/TOR-FoxO3a signaling pathway and can improve muscle texture and nutritional composition (H. Yang, Li, Rahman, & Leng, 2023). In the present study, the SG73 group was enriched for more beneficial AA through the upregulation biosynthesis of amino acids pathway compared to the WG group. Therefore, it was speculated that the quality of black Tibetan sheep was more in line with human requirements.

Based on 16S rDNA amplicon sequencing, 1700 and 838 OTUs were identified for WG and SG73, respectively, but there were no significant differences in rumen microbial diversity between the two groups. All the samples were dominated by *Bacteroidetes* and *Firmicutes*. These findings are consistent with those obtained by Y.K. Zhang et al (Y. K. Zhang et al., 2021) during the study of sheep rumen microbiota. It was speculated that rumen microorganisms may indirectly affect the deposition of metabolites through interactions with the host (B. Wang et al., 2021). Rumen beneficial bacteria are closely related to metabolites such as AA and FA in meat nutrients, and are involved in lipid metabolism. Interestingly, the relative abundance of *Christonsenellaceas R-7*, *Alistipes* and other genera differed significantly between the two groups, and these differentially abundant bacteria may affect the composition of AA and FA, while improving the production of some beneficial metabolites such as D-Fructose-6-phosphate, D-glucose 6-phosphate and Argininosuccinic acid. *Akkermansia* can regulate fat storage and energy metabolism, maintain mucosal immunity, and have an anti-obesity effect(Longo, Frigeni, & Pasquali). *Lachnospiraceae* is a soluble polysaccharide degrading bacterium(C. Yang, Wang, Deng, & Huang, 2021). But currently there is still a paucity of confirmation to support the association between most beneficial compounds, including meat quality, AA, FA, and rumen microorganisms.

Based on the overall evaluation, it was speculated that the meat of the black Tibetan sheep could be of better quality. AA and FA metabolism of Tibetan sheep in the SG73 group were also influenced and these further regulated epigenetic characteristics, such as WBSF and cooking loss, to improve the nutritional quality of black Tibetan sheep. Most of the results in targeted and non-targeted metabolomics were consistent with those of AA and FA. However, further investigation is needed to explain the changes in non-target metabolites as well as changes in metabolic pathways from the perspective of rumen microorganisms and thus meat quality differences (Fig. 6).

5. Conclusions

The results suggest that identification of non-target metabolites in muscle and microbiota in the rumen could further provide useful information for understanding meat quality changes of Tibetan sheep. In this study, the Tibetan sheep of SG73 group had excellent water holding capacity, tender, lower fat content and higher AA level compared with the WG group. While meat quality and metabolite correlation analysis showed that the WBSF, color and water holding capacity of meat were closely linked to metabolites such as D-glucose 6-phosphate, and that these characteristics were regulated through a number of potential

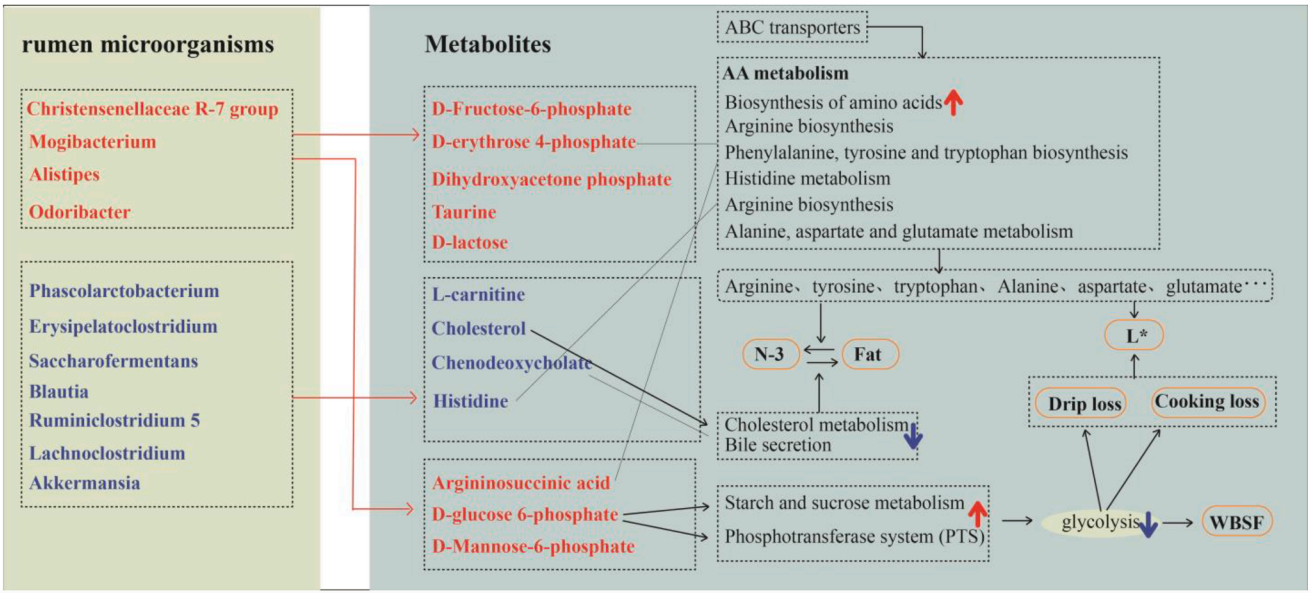

Fig. 6. Hypothesized scheme pathways and microbial function related to the changes of the microbiome in the rumen and metabolome in the *longissimus dorsi* muscles. Metabolites and bacteria in blue and red indicate them down regulated and up regulated significantly with SG73 compared to WG group, respectively ($P < 0.05$). Red and black arrows indicate up-regulation and down-regulation of metabolic pathways, respectively ($P < 0.05$). The red line denotes the significantly positive correlation between these two items. The full black line with the arrow(s) denotes a metabolic relationship and direction between every two substances.

pathways associated with glycolysis, such as phosphotransferase system. What more, cholesterol metabolism is a potential pathway regulating fat deposition. And in the analysis of the correlation between gut microbes and meat quality and metabolites, it was found that gut microbes influence muscle metabolites through sugar metabolism and amino acid metabolism in the rumen, which in turn regulates meat quality. However, further research is required to investigate the specific regulatory molecular mechanism. This could provide a theoretical basis for further investigation into the regulatory mechanisms of meat quality, as well as help to promote the development of high-quality Tibetan sheep in the region.

Funding: The current work was funded by Evaluation and Analysis of Nutritional Value of Black Tibetan Sheep and Research on Development of Series Products Funds of Qinghai Province (2020-GN-119) and Construction of Standardized Production System for Improving quality and efficiency of Tibetan sheep industry (2022-NK-169).

Data availability: The raw data of this study are derived from the GEO data portal (https://www.ncbi.nlm.nih.gov/geo/), which are publicly available databases, where the 16 s rDNA raw data record number: PRJNA899005 (Release 2023.1.02), and the Metabolights Raw data accession number is: MTBLS6424 (Release 2023.11.8).

Ethics approval and consent to participate: This study was carried out in strict accordance with the animal protection and use guidelines established by the Ministry of Science and Technology of the People's Republic of China. All animal care and handling were approved by the Institutional Animal Care and Use Committee Guidelines of Qinghai University (protocol number 0515). Moreover, all applicable rules and regulation of the organization and government were followed regarding the ethical use of experimental animals.

Consent for publication: Not applicable.

CRediT authorship contribution statement

Ying Ma: Conceptualization, Data curation, Formal analysis, Methodology, Software, Validation, Visualization, Writing – original draft. **Lijuan Han:** Conceptualization, Formal analysis, Funding acquisition, Methodology, Project administration, Supervision, Writing – original draft, Writing – review & editing. **Shutong Zhang:** Formal analysis. **Xue Zhang:** Conceptualization, Visualization. **Shengzhen Hou:** Conceptualization, Investigation, Resources, Validation. **Linsheng Gui:** Software. **Shengnan Sun:** . **Zhenzhen Yuan:** Data curation, Software. **Zhiyou Wang:** Investigation. **Baochun Yang:** Formal analysis, Investigation.

Declaration of Competing Interest

The authors declare that they have no known competing financial interests or personal relationships that could have appeared to influence the work reported in this paper.

Data availability

I have share the link to my data

Acknowledgements

The authors acknowledge Xingang Lv(Shanghai Applied Protein Technology Co., Ltd., China) for the technical support. The authors are thankful to the support of Qinghai University for the use of laboratory facilities.

Appendix A. Supplementary data

Supplementary data to this article can be found online at https://doi.org/10.1016/j.fochx.2023.100843.

References

Arena, S., Salzano, A. M., Renzone, G., D'Ambrosio, C., & Scaloni, A. (2014). Non-enzymatic glycation and glycoxidation protein products in foods and diseases: An interconnected, complex scenario fully open to innovative proteomic studies. *Mass Spectrometry Reviews, 33*(1), 49–77.

Atsbha, K., Gebremariam, T., & Aregawi, T. (2021). Slaughter performance and meat quality of Begait breed lambs fattened under different diets. *Heliyon, 7*(5), e06935.

Ayub, H., & Ahmad, A. (2019). Physiochemical changes in sous-vide and conventionally cooked meat. *International journal of gastronomy and food science, 17*, Article 100145.

Białek, M., Czauderna, M., & Białek, A. (2018). Partial replacement of rapeseed oil with fish oil, and dietary antioxidants supplementation affects concentrations of biohydrogenation products and conjugated fatty acids in rumen and selected lamb tissues. *Animal Feed Science and Technology, 241*, 63–74. https://doi.org/10.1016/j.anifeedsci.2018.04.015

Borges, B. O., Curi, R. A., Baldi, F., Feitosa, F. L. B., Andrade, W. B. F. d., Albuquerque, L. G. d., . . . Chardulo, L. A. L. (2014). Polymorphisms in candidate genes and their association with carcass traits and meat quality in Nellore cattle. *Pesquisa Agropecuaria Brasileira, 49*(5), 364-371.

Cabaton, N. J., Poupin, N., Canlet, C., Tremblay-Franco, M., Audebert, M., Cravedi, J.-P., … Zalko, D. (2018). An untargeted metabolomics approach to investigate the metabolic modulations of HepG2 cells exposed to low doses of bisphenol A and 17β-estradiol. *Frontiers in Endocrinology, 571*.

Calderón, C., & Lämmerhofer, M. (2022). Enantioselective metabolomics by liquid chromatography-mass spectrometry. *Journal of Pharmaceutical and Biomedical Analysis, 207*, Article 114430.

Caporaso, J. G., Kuczynski, J., Stombaugh, J., Bittinger, K., Bushman, F. D., Costello, E. K., … Gordon, J. I. (2010). QIIME allows analysis of high-throughput community sequencing data. *Nature methods, 7*(5), 335–336.

Chen, C., Guo, Z., Shi, X., Guo, Y., Ma, G., Ma, J., & Yu, Q. (2022). H2O2-induced oxidative stress improves meat tenderness by accelerating glycolysis via hypoxia-inducible factor-1α signaling pathway in postmortem bovine muscle. *Food Chemistry: X, 16*, Article 100466. https://doi.org/10.1016/j.fochx.2022.100466

Cobellis, G., Trabalza-Marinucci, M., & Yu, Z. (2016). Critical evaluation of essential oils as rumen modifiers in ruminant nutrition: A review. *Science of The Total Environment, 545–546*, 556–568. https://doi.org/10.1016/j.scitotenv.2015.12.103

Colucci, P. E., Macleod, G. K., Grovum, W. L., McMillan, I., & Barney, D. J. (1990). Digesta Kinetics in Sheep and Cattle Fed Diets with Different Forage to Concentrate Ratios at High and Low Intakes. *Journal of Dairy Science, 73*(8), 2143–2156. https://doi.org/10.3168/jds.S0022-0302(90)78895-9

Devapriya, A., Sejian, V., Ruban, W., Devaraj, C., Spandan, P. V., Silpa, M. V., … Bhatta, R. (2021). Analysis of carcass traits and quantitative expression patterns of different meat quality governing genes during heat stress exposure in indigenous goats. *Food Chemistry: Molecular Sciences, 3*, Article 100052.

Du, M., Yang, C., Liang, Z., Zhang, J., Yang, Y., Ahmad, A. A., . . . Ding, X. J. F. i. v. s. (2021). Dietary Energy Levels Affect Carbohydrate Metabolism-Related Bacteria and Improve Meat Quality in the. *8*, 718036.

Egelandsdal, B., Berg, P., Wahlgren, M., & Slinde, E. (2016). Glutamine and succinate stabilize shelf-life color of frozen and thawed meat by stimulation of mitochondrial respiration. *Meat science, 112*, 137. https://doi.org/10.1016/j.meatsci.2015.08.083

Fiehn, O. (2002). Metabolomics—the link between genotypes and phenotypes. *Functional genomics*, 155–171.

Guerreiro, O., Francisco, A. E., Alves, S. P., Soldado, D., Cachucho, L., Chimenos, A. U., … Jerónimo, E. (2022). Inclusion of the aerial part and condensed tannin extract from Cistus ladanifer L. in lamb diets – Effects on rumen microbial community and fatty acid profile. *Animal Feed Science and Technology, 291*, Article 115398. https://doi.org/10.1016/j.anifeedsci.2022.115398

Gui, L.-S., Raza, S. H. A., Ahmed Allam, F. A. E., Zhou, L., Hou, S., Khan, I., … Wang, Z. (2021). Altered milk yield and rumen microbial abundance in response to concentrate supplementation during the cold season in Tibetan sheep. *Electronic Journal of Biotechnology, 53*, 80–86. https://doi.org/10.1016/j.ejbt.2021.07.001

Guo, W., Guo, X. J., Xu, L. N., Shao, L. W., Zhu, B. C., Liu, H., … Gao, K. Y. (2022). Effect of whole-plant corn silage treated with lignocellulose-degrading bacteria on growth performance, rumen fermentation, and rumen microflora in sheep. *Animal, 16*(7), Article 100576. https://doi.org/10.1016/j.animal.2022.100576

Gurgul, A., Jasielczuk, I., Miksza-Cybulska, A., Kawęcka, A., Szmatoła, T., & Krupiński, J. (2021). Evaluation of genetic differentiation and genome-wide selection signatures in Polish local sheep breeds. *Livestock Science, 251*, Article 104635. https://doi.org/10.1016/j.livsci.2021.104635

Han, J.-L., Min, Y., Guo, T.-T., Yue, Y.-J., Liu, J.-B., Niu, C.-E., … Yang, B.-H. (2015). Molecular characterization of two candidate genes associated with coat color in Tibetan sheep (Ovis arise). *Journal of integrative agriculture, 14*(7), 1390–1397.

Harlioğlu, M. M., Köprücü, K., Harlioğlu, A. G., Yilmaz, Ö., Aydin, S., Mişe Yonar, S., … Özcan, S. (2012). The effects of dietary n−3 series fatty acid on the fatty acid composition, cholesterol and fat-soluble vitamins of pleopodal eggs and stage 1 juveniles in a freshwater crayfish, Astacus leptodactylus (Eschscholtz). *Aquaculture, 356–357*, 310–316. https://doi.org/10.1016/j.aquaculture.2012.05.001

Honikel, K. O. (1998). Reference methods for the assessment of physical characteristics of meat. *Meat science, 49*(4), 447–457.

Jiao, J., Wang, T., Zhou, J., Degen, A. A., Gou, N., Li, S., … Shang, Z. (2020). Carcass parameters and meat quality of Tibetan sheep and Small-tailed Han sheep consuming diets of low-protein content and different energy yields. *Journal of Animal Physiology and Animal Nutrition, 104*(4), 1010–1023.

Jing, X. P., Wang, W. J., Degen, A. A., Guo, Y. M., Kang, J. P., Liu, P. P., … Long, R. J. (2022). Small intestinal morphology and sugar transporters expression when consuming diets of different energy levels: Comparison between Tibetan and small-tailed Han sheep. *Animal, 16*(3), Article 100463. https://doi.org/10.1016/j.animal.2022.100463

Kanehisa, M. (2019). Toward understanding the origin and evolution of cellular organisms. *Protein Science, 28*(11), 1947–1951.

Kanehisa, M., Furumichi, M., Sato, Y., Ishiguro-Watanabe, M., & Tanabe, M. (2021). KEGG: Integrating viruses and cellular organisms. *Nucleic Acids Research, 49*(D1), D545–D551.

Kanehisa, M., & Goto, S. (2000). KEGG: Kyoto encyclopedia of genes and genomes. *Nucleic acids research, 28*(1), 27–30.

Knowles, S. O., Grace, N. D., Rounce, J. R., & Realini, C. E. (2020). Quality, nutrient and sensory characteristics of aged meat from lambs supplemented with selenomethionine. *Food Research International, 137*, Article 109655.

Langille, M. G. I., Zaneveld, J., Caporaso, J. G., McDonald, D., Knights, D., Reyes, J. A., … Knight, R. (2013). Predictive functional profiling of microbial communities using 16S rRNA marker gene sequences. *Nature biotechnology, 31*(9), 814–821.

Lee, S. M., Kwon, G. Y., Kim, K.-O., & Kim, Y.-S. (2011). Metabolomic approach for determination of key volatile compounds related to beef flavor in glutathione-Maillard reaction products. *Analytica Chimica Acta, 703*(2), 204–211. https://doi.org/10.1016/j.aca.2011.07.028

Ley, R. E., Turnbaugh, P. J., Klein, S., & Gordon, J. I. (2006). Human gut microbes associated with obesity. *Nature, 444*(7122), 1022–1023. https://doi.org/10.1038/4441022a

Li, H., Mi, Y., Duan, Z., Ma, P., & Fan, D. (2020). Structural characterization and immunomodulatory activity of a polysaccharide from Eurotium cristatum. *International Journal of Biological Macromolecules, 162*, 609–617. https://doi.org/10.1016/j.ijbiomac.2020.06.099

Li, Q., Hakimi, P., Liu, X., Yu, W.-M., Ye, F., Fujioka, H., … Dunwoodie, S. L. (2014). Cited2, a transcriptional modulator protein, regulates metabolism in murine embryonic stem cells. *Journal of Biological Chemistry, 289*(1), 251–263.

Liu, Q., Long, Y., Zhang, Y. F., Zhang, Z. Y., Yang, B., Chen, C. Y., … Su, Y. (2021). Phenotypic and genetic correlations of pork myoglobin content with meat colour and other traits in an eight breed-crossed heterogeneous population. *Animal, 15*(11), Article 100364. https://doi.org/10.1016/j.animal.2021.100364

Matthews, C., Crispie, F., Lewis, E., Reid, M., O'Toole, P. W., & Cotter, P. D. (2019). The rumen microbiome: A crucial consideration when optimising milk and meat production and nitrogen utilisation efficiency. *Gut Microbes, 10*(2), 115–132. https://doi.org/10.1080/19490976.2018.1505176

Miller, R. K. (2023). The eating quality of meat: V Sensory evaluation of meat. In *Lawrie's meat science* (pp. 509–548). Elsevier.

Palka, K., & Daun, H. (1999). Changes in texture, cooking losses, and myofibrillar structure of bovine M. semitendinosus during heating. *Meat science, 51*(3), 237–243. https://doi.org/10.1016/S0309-1740(98)00119-3

Purslow, P. P., Gagaoua, M., & Warner, R. D. (2021). Insights on meat quality from combining traditional studies and proteomics. *Meat science, 174*, Article 108423. https://doi.org/10.1016/j.meatsci.2020.108423

Qiao, M., Fletcher, D. L., Smith, D. P., & Northcutt, J. K. (2001). The Effect of Broiler Breast Meat Color on pH, Moisture, Water-Holding Capacity, and Emulsification Capacity. *Poultry Science, 80*(5), 676–680. https://doi.org/10.1093/ps/80.5.676

Sadet-Bourgeteau, S., Martin, C., & Morgavi, D. P. (2010). Bacterial diversity dynamics in rumen epithelium of wethers fed forage and mixed concentrate forage diets. *Veterinary Microbiology, 146*(1), 98–104. https://doi.org/10.1016/j.vetmic.2010.04.029

Scott, A. L. (1939). How much fat do consumers want in beef? *Journal of Animal Science, 1939*(1), 103–107.

Shi, M. J., Ma, Z. X., Tian, Y. J., Ma, C., Li, Y. D., & Zhang, X. W. (2022). Effects of corn straw treated with CaO on rumen degradation characteristics and fermentation parameters and their correlation with microbial diversity in rumen. *Animal Feed Science and Technology, 292*, Article 115403. https://doi.org/10.1016/j.anifeedsci.2022.115403

Stahl, C. A., Carlson-Shannon, M. S., Wiegand, B. R., Meyer, D. L., Schmidt, T. B., & Berg, E. P. (2007). The influence of creatine and a high glycemic carbohydrate on the growth performance and meat quality of market hogs fed ractopamine hydrochloride. *Meat science, 75*(1), 143–149. https://doi.org/10.1016/j.meatsci.2006.06.023

STANDARD, B., & ISO, B. (2003). Sensory analysis—Methodology—General guidance for establishing a sensory profile.

Sun, Y. K., Yan, X. G., Ban, Z. B., Yang, H. M., Hegarty, R. S., & Zhao, Y. M. (2017). The effect of cysteamine hydrochloride and nitrate supplementation on in-vitro and in-vivo methane production and productivity of cattle. *Animal Feed Science and Technology, 232*, 49–56.

Thompson, J. M. (2004). The effects of marbling on flavour and juiciness scores of cooked beef, after adjusting to a constant tenderness. *Australian Journal of Experimental Agriculture, 44*(7), 645–652.

Tian, F., Decker, E. A., & Goddard, J. M. (2013). Controlling lipid oxidation of food by active packaging technologies. *Food & function, 4*(5), 669–680.

Wang, B., Wang, Y., Zuo, S., Peng, S., Wang, Z., Zhang, Y., & Luo, H. (2021). Untargeted and Targeted Metabolomics Profiling of Muscle Reveals Enhanced Meat Quality in Artificial Pasture Grazing Tan Lambs via Rescheduling the Rumen Bacterial Community. *Journal of Agricultural and Food Chemistry, 69*(2), 846–858. https://doi.org/10.1021/acs.jafc.0c06427

Wang, X., Xu, T., Zhang, X., Zhao, N., Hu, L., Liu, H., . . . Xu, S. (2022). The Response of Ruminal Microbiota and Metabolites to Different Dietary Protein Levels in Tibetan Sheep on the Qinghai-Tibetan Plateau. (2297-1769 (Print)).

Weimer, P. J., Waghorn, G. C., Odt, C. L., & Mertens, D. R. (1999). Effect of Diet on Populations of Three Species of Ruminal Cellulolytic Bacteria in Lactating Dairy Cows1. *Journal of Dairy Science, 82*(1), 122–134. https://doi.org/10.3168/jds.S0022-0302(99)75216-1

Wikoff, W. R., Anfora, A. T., Liu, J., Schultz, P. G., Lesley, S. A., Peters, E. C., & Siuzdak, G. (2009). Metabolomics analysis reveals large effects of gut microflora on mammalian blood metabolites. *Proceedings of the national academy of sciences, 106*(10), 3698-3703.

Wright André-Denis, G., Williams Andrew, J., Winder, B., Christophersen Claus, T., Rodgers Sharon, L., & Smith Kellie, D. (2004). Molecular Diversity of Rumen Methanogens from Sheep in Western Australia. *Applied and environmental microbiology, 70*(3), 1263–1270. https://doi.org/10.1128/AEM.70.3.1263-1270.2004

Xiang, J., Zhong, L., Luo, H., Meng, L., Dong, Y., Qi, Z., & Wang, H. (2022). A comparative analysis of carcass and meat traits, and rumen bacteria between Chinese Mongolian sheep and Dorper × Chinese Mongolian crossbred sheep. *Animal, 16*(4), Article 100503. https://doi.org/10.1016/j.animal.2022.100503

Xing, B.-S., Han, Y., Wang, X. C., Wen, J., Cao, S., Zhang, K., … Yuan, H. (2020). Persistent action of cow rumen microorganisms in enhancing biodegradation of wheat straw by rumen fermentation. *Science of The Total Environment, 715*, Article 136529. https://doi.org/10.1016/j.scitotenv.2020.136529

Yang, C., Wang, X., Deng, Q., & Huang, F. (2021). Rapeseed polysaccharides alleviate overweight induced by high-fat diet with regulation of gut microbiota in rats. *Oil Crop Science, 6*(4), 192–200. https://doi.org/10.1016/j.ocsci.2021.09.001

Yang, H., Li, X., Rahman, M. M., & Leng, X. (2023). Dietary supplementation of leucine improved the flesh quality of largemouth bass, Micropterus salmoides through TOR, FoxO3a and MRFs regulation. *Aquaculture, 566*, Article 739237. https://doi.org/10.1016/j.aquaculture.2023.739237

Zhang, X., Han, L., Gui, L., Raza, S. H. A., Hou, S., Yang, B., … Ibrahim, S. F. (2023). Metabolome and microbiome analysis revealed the effect mechanism of different feeding modes on the meat quality of Black Tibetan sheep. *Frontiers in Microbiology, 13*, Article 1076675. https://doi.org/10.3389/fmicb.2022.1076675

Zhang, X., Han, L., Hou, S., Raza, S. H. A., Gui, L., Sun, S., . . . Aloufi, B. H. (2022). Metabolomics approach reveals high energy diet improves the quality and enhances the flavor of black Tibetan sheep meat by altering the composition of rumen microbiota. (2296-861X (Print)).

Zhang, X., Han, L., Hou, S., Raza, S. H. A., Wang, Z., Yang, B., . . . Al Hazani, T. M. I. (2022). Effects of different feeding regimes on muscle metabolism and its association with meat quality of Tibetan sheep. (1873-7072 (Electronic)).

Zhang, Y. K., Zhang, X. X., Li, F. D., Li, C., Li, G. Z., Zhang, D. Y., … Wang, W. M. (2021). Characterization of the rumen microbiota and its relationship with residual feed intake in sheep. *Animal, 15*(3), Article 100161. https://doi.org/10.1016/j.animal.2020.100161

Zheng, H., Zhao, T., Xu, Y.-C., Zhang, D.-G., Song, Y.-F., & Tan, X.-Y. (2022). Dietary choline prevents high fat-induced disorder of hepatic cholesterol metabolism through SREBP-2/HNF-4α/CYP7A1 pathway in a freshwater teleost yellow catfish Pelteobagrus fulvidraco. *Biochimica et Biophysica Acta (BBA) - Gene Regulatory Mechanisms, 1865*(7), Article 194874. https://doi.org/10.1016/j.bbagrm.2022.194874